A&A manuscript no.
(will be inserted by hand later)

Your thesaurus codes are:
08 (08.01.1; 08.01.3; 08.09.2 NGC 6751; 08.09.2 Sand 3 ; 08.13.2; 08.23.2)

ASTRONOMY
AND
ASTROPHYSICS
30.7.1996

Spectral analyses of central stars of planetary nebulae of early WC-type ⋆

NGC 6751 and Sanduleak 3

L. Koesterke and W.-R. Hamann

Lehrstuhl Astrophysik, Universität Potsdam, Am Neuen Palais 10, D-14469 Potsdam, Germany
e-mail (L.K.): lars@astro.physik.uni-potsdam.de

Received date; accepted date

Abstract. The two Wolf-Rayet type central stars of the planetary nebulae NGC 6751 and Sanduleak 3, showing the early spectral subtypes [WC 4] and [WC 2-3], respectively, are analyzed by means of non-LTE models for spherically expanding atmospheres. Complex model atoms of helium, carbon, oxygen and nitrogen are taken into account. For the atmospheric composition we find a carbon-to-helium mass ratio of about 0.5 in both stars. The oxygen mass fraction is about 0.15 ± 0.1. The nitrogen abundance in Sand 3 is about 0.005. In NGC 6751 nitrogen is also clearly present but a quantitative determination failed. The parameter T_*, defined as the effective temperature related to the stellar core radius, is about 140 kK for both stars. Adopting a luminosity of $5000\,L_\odot$, the stellar radii and mass-loss rates are determined (NGC 6751: $0.13\,R_\odot$, $10^{-6.1}$ ... $10^{-5.5}$ $M_\odot\,\mathrm{yr}^{-1}$, Sand 3: $0.12\,R_\odot$, $10^{-6.15}$ $M_\odot\,\mathrm{yr}^{-1}$). From the spread of ionization stages in the optical spectrum of NGC 6751 we find hints for inhomogeneities in the atmosphere and estimate a density contrast of 0.6 dex. The stellar evolution is discussed with regard to recently analyzed PG 1159 and late-type [WC] stars. The results of our analyses are in rough accordance with the "born-again scenario" and suggest an evolutionary path [WC-late] → [WC-early] → PG 1159. In conflict is the carbon abundance, as we derive lower values than found in [WC-late] and PG 1159 stars.

Key words: stars: Wolf-Rayet – stars: atmospheres – stars: abundances – stars: mass-loss – stars: individual: NGC 6751, Sand 3

1. Introduction

Central stars of planetary nebulae (CSPN) whose spectra are dominated by strong emission lines are termed as Wolf-Rayet (WR) stars, in analogy to their massive Population I counterparts. Early papers (e.g. Perek & Kohoutek 1967) have distributed the WR-CSPN over both subclasses, the nitrogen (WN) and the carbon (WC) sequence, according to the suggested dominance of nitrogen and carbon emission lines, respectively. Meanwhile it became clear on the basis of better spectra that, apart from one or two exceptions, all known WR-type CSPN belong to the carbon sequence. This class of CSPN, in contrast to the Pop. I WC class termed [WC] with brackets (van der Hucht et al. 1981), is arranged in a subtype sequence [WC 2] to [WC 12] reflecting the degree of ionization. [WC 2] to [WC 6] are called "early", [WC 7] to [WC 12] are termed "late" subtypes. This is similar to the classification system for Pop. I WC stars. One difference is that no particular WO class (oxygen sequence) is introduced for the earliest subtypes of [WC] central stars. The distribution of the [WC] stars over the subclasses is strikingly different from the Pop. I WC stars. For a review about the [WC] class and their spectra see e.g. Hamann (1996).

A major motivation for studying [WC]-type central stars is to establish empirical constraints for the various scenarios of post-AGB evolution. Related objects are the PG 1159 stars, which seem to have a similar surface composition (helium, carbon, oxygen, traces of nitrogen, but no detectable hydrogen, cf. Dreizler et al. 1995b), but do not show mass-loss. Weak but visible mass-loss is indicated by the intermediate spectral class [WC]-PG 1159. The favored explanation for the surface compositions of these related stars is provided by the "born-again scenario" (Iben et al. 1983).

In order to derive closer constraints to the evolutionary status of the [WC] stars, an empirical determination of their parameters and chemical composition is required. However, due to the velocity field and the extreme non-LTE conditions, an

---

Send offprint requests to: L. Koesterke

⋆ Partly based on observations obtained at the German–Spanish Astronomical Center, Calar Alto, Spain adequate modelling of these expanding stellar atmospheres is difficult.

In the last years we started to apply our program code, which was originally developed for analyzing massive WR stars, to central stars as well. One [WC 12] star (V 348 Sgr) has been investigated by Leuenhagen & Hamann (1994). Surprisingly, they detected traces of hydrogen and an unexpectedly large amount of nitrogen in its atmosphere which is predominantly composed of carbon and helium. Analyses of further seven late-type [WC] stars were published recently (Leuenhagen et al. 1996).

The studies of two early-type [WC] stars have been presented in two conference papers in preliminary form (NGC 6751: Hamann & Koesterke 1992; WR 72: Koesterke & Hamann 1995). Note that Sanduleak 3 was originally included as "WR 72" in the catalogue of Pop. I Galactic Wolf-Rayet stars (van der Hucht et al. 1981), but later reclassified as a CSPN (van der Hucht & Williams 1987) and excluded in the current Pop. I catalogue version (van der Hucht et al. 1988). In the present work we present the analyses of these two stars in detail. Further analyses of [WC] stars in the Galaxy and the Magellanic Clouds are planned for the future.

In Sect. 2 we briefly describe the model calculations and the model atoms applied. The observations are presented in Sect. 3, followed by the analyses of the two stars including detailed comparisons between the observed and the synthetic spectra (Sect. 4). Finally we discuss the results and draw some conclusions concerning the evolutionary status of the two stars (Sect. 5).

2. Model atmospheres

The model calculations are very similar to those described in previous papers (Koesterke et al. 1992, Hamann et al. 1992, Koesterke & Hamann 1995, Leuenhagen & Hamann 1994, Leuenhagen et al. 1996). The standard model assumptions of spherically symmetric outflow, homogeneity and stationarity are adopted. The radiation transfer is calculated in the co-moving frame under non-LTE conditions, accounting for complex model atoms. Each model is specified by its stellar temperature T_*, stellar radius R_*, mass-loss rate $\dot{M}$ and the terminal velocity v_∞.

Moreover, the chemical abundances of carbon, nitrogen and oxygen are specified (as mass-fractions β_C, β_N, β_O), while the rest is contributed by helium. The model atoms contain numerous levels of the important ionization stages (i.e. He I, He II, C II-C IV, N IV, N V, O III-O VI) and a few levels of adjacent stages. A summarizing description of the model atoms is given in Table 1.

The so-called ALI formalism (accelerated lambda iteration, cf. Hamann 1985, 1986, 1987) is applied for the consistent solution of the radiation transfer and the statistical equilibrium equations. Finally, after the source function has been calculated, the radiation transfer is solved in the observer's frame and the emergent flux is derived (Formal Integral). Those levels composed of different angular momentum substates are split into their components at that stage assuming relative LTE population. Moreover the frequency redistribution of line photons by Thomson scattering is accounted for in the Formal Integral, as suggested by Hillier (1991) and adapted to our code by Hamann et al. (1992).

Table 1. Summary of the model atoms

Ion	Sand 3 Levels	NGC 6751 Levels
He I	17	17
He II	16	16
He III	1	1
C I	-	2
C II	3	32
C III	40	40
C IV	19	19
C V	1	1
N III	1	-
N IV	38	-
N V	19	-
N VI	1	-
O II	-	3
O III	1	33
O IV	25	25
O V	36	36
O VI	15	15
O VII	1	1
total	234	241

We introduce the so-called transformed radius R_t, which can be interpreted as a density parameter, connecting R_*, $\dot{M}$ and v_∞ via the transformation law

$$R_\mathrm{t} = R_* \left[\frac{v_\infty}{2500\,\mathrm{km\,s^{-1}}} \Big/ \frac{\dot{M}}{10^{-4}\,M_\odot\,\mathrm{yr^{-1}}} \right]^{2/3} . \qquad (1)$$

Under the condition of fixed abundances, two models with the same T_* and R_t show very similar spectra irrespective of the individual values of R_*, $\dot{M}$ and v_∞ (Schmutz et al. 1989). Especially the line equivalent widths are nearly independent of the individual combination of these quantities.

While the blanketing effect of the numerous carbon and oxygen lines is included in our models, metal line blanketing is neglected so far. Due to pilot studies (Schmutz 1991, Hillier in prep.) the expected impact on the results is only moderate.

3. The observations

3.1. NGC 6751

The central star of NGC 6751, alias HD 177656, has been observed by us during the observation run between June 24 and July 1, 1991, at the "Deutsch-Spanisches Astronomisches Zentrum (DSAZ)", Calar Alto, Spain. We used the 2.2 m telescope with the Boller & Chivens spectrograph and a coated CCD (GEC). Three exposures were made, covering the wide spectral range between 3320 Å and 7400 Å. The spectral resolution is about 3600.

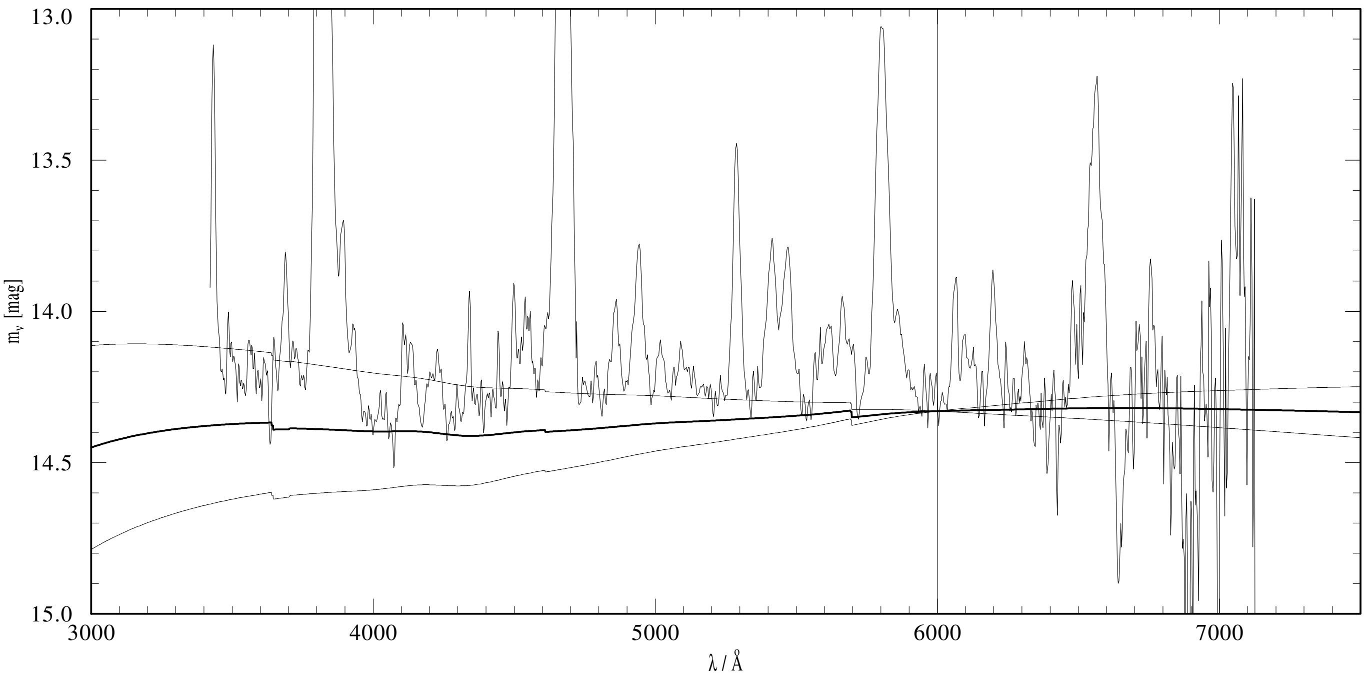

Fig. 1. Spectrophotometric observation of Sand 3 together with the synthetic continuum reddened with $E_{\rm b-v}$ = 0.23, 0.43 (thin lines) and $E_{\rm b-v}$ = 0.33 (thick line). The three continua are scaled to the observed flux at the line-free range around 6000 Å. The continuum reddened with $E_{\rm b-v}$ = 0.33 fairly agrees with the slope of the observed spectrum between 3420 Å and 6250 Å. The redmost 500 Å of the observation are underexposed.

The three spectra were extracted using software written in Kiel by G. Jonas. After division by a fit to the continuum of a standard star, low-order polynominals were adjusted "by eye" to the continuum of NGC 6751 yielding flux-normalized spectra. Finally the three spectra were joined together.

The low resolution IUE spectra SWP 14179 and SWP 14180 are taken from the GSFC data base. Unfortunately the wavelength axis of both spectra is damaged, and we tried to restore it by an estimated shift of about 145 Å. The continuum for the rectification of the IUE spectra was drawn by eye.

The spectrum differs remarkably from those of other [WC 4]-CSPNs like IC 1747 and NGC 1501. The lines are exceptionally strong and in addition C III at 5696 Å is visible. The spectrum rather resembles the Pop. I WC 5 star WR 111.

3.2. Sand 3

The spectrum of Sand 3 is taken from the atlas of optical spectrophotometry of Torres & Massey (1987). The resolution is about 8 Å. Similar as Koesterke & Hamann (1995) we reduced uncertainties concerning the proper choice of the continuum by improving the spectrum rectification iteratively during the progress of the analysis. This is illustrated in Fig. 1.

In Fig. 1 the spectrum of Sand 3 is drawn together with the synthetic spectrum reddened with $E_{\rm b-v}$ = 0.23, 0.33 and 0.43, respectively. Note that the flux is plotted on the magnitude scale m_ν, using the calibration of Vega by Hayes & Latham (1975). The three continua are adjusted to the stellar flux at 6000 Å where no lines appear to contaminate the stellar continuum. The synthetic continuum, reddened with $E_{\rm b-v}$ = 0.33, fairly represents the slope of the spectrum from the blue edge up to 6250 Å. To obtain the normalized spectrum we finally divide the observed flux by the model flux. In the redmost 500 Å the stellar signal is noisy and therefore disregarded.

Additionally to the optical data the low resolution IUE spectrum SWP 6773 (exposure time 75 min) was retrieved from the GSFC data base. This observation was rectified by eye to obtain a flux-normalized spectrum.

The spectrum looks similar to those of NGC 5189 ([WC 2]) and PB 6 ([WC 3]). In the optical range the spectra of these three stars are dominated by the very strong O VI line at 3820 Å. In the UV the strongest lines are the C IV 1548, 1550 Å resonance doublet, He II 1640 Å, O V 1371 Å, and the N V 1238, 1242 Å resonance doublet. Thus Sand 3 is a typical representative of [WC]-CSPNs with very early subtype. Compared to Pop. I WO stars the line strengths are similar, while the line widths are smaller (e.g. Torres & Massey 1987, their figure 8). However, the N V resonance line is more dominant in the UV, compared to typical Pop. I WC spectra.

4. Analyses

For both stars the distance is not known, and hence the luminosity can not be deduced from the spectroscopic analyses. Instead we adopt a value of $\log{(L/L_\odot)}$ = 3.7. According to evolutionary calculations (e.g. Schönberner 1983) this is a typical value

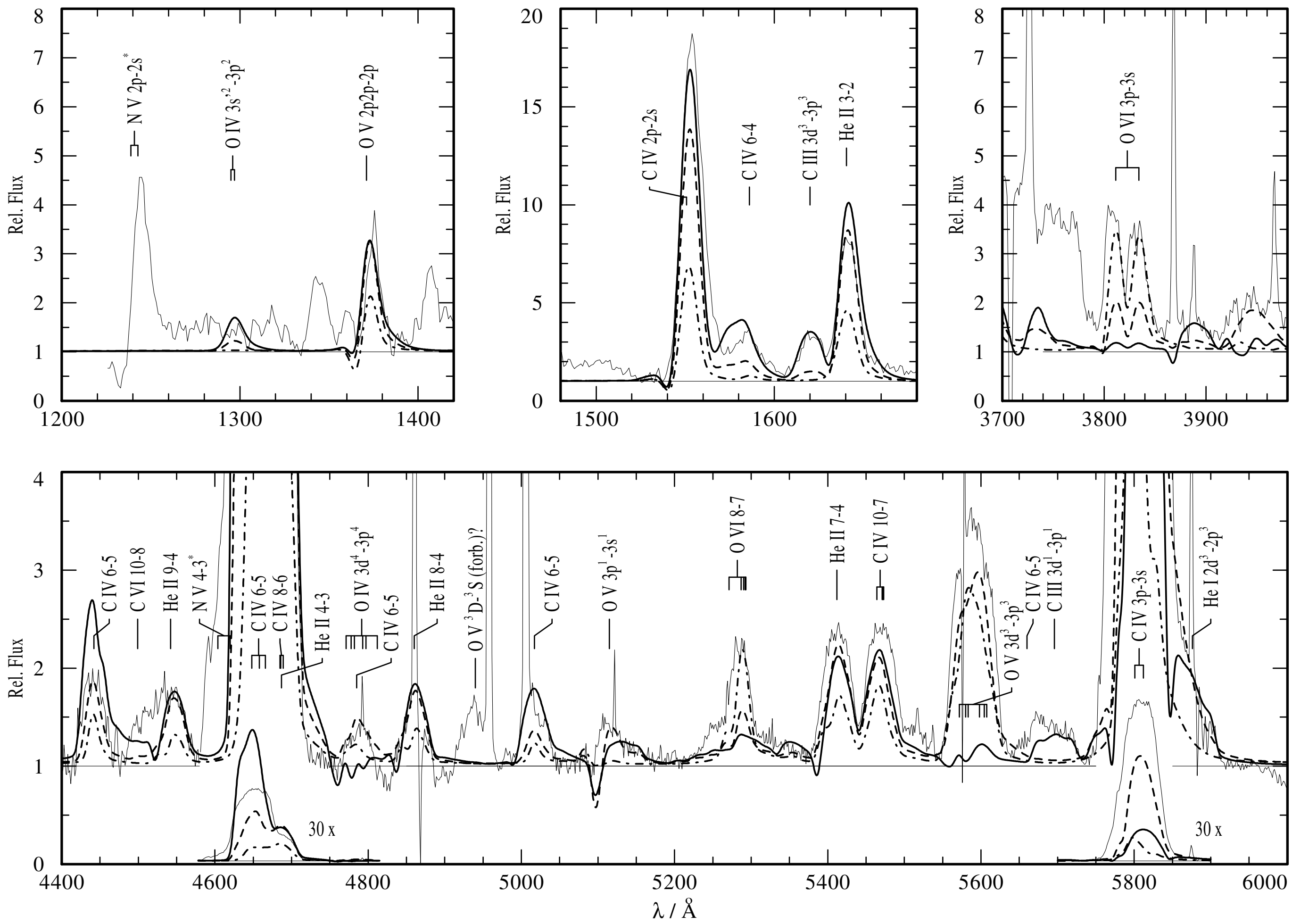

Fig. 2. Spectral fit of NGC 6751. The observation (thin lines) is shown together with synthetic spectra of three models (thick lines) which differ in the mass-loss rate only. The solid line shows the model with the high mass-loss rate ($10^{-5.52}\ M_\odot\ \mathrm{yr}^{-1}$), the dashed line the intermediate model ($10^{-5.97}$) and the dashed-dotted line the model with the low mass-loss rate ($10^{-6.12}$). The further model parameters are given in Table 2. The three different models are necessary to reproduce the observed wide spread of ionization stages. The lines of the low ionization stages (C III and He I) are fitted by the model with the high mass-loss rate, while the lines of the intermediate ionization stages (He II, C IV and O V) are reproduced by both the models with the intermediate and the low transformed radius. The model with the high transformed radius additionally fits the O VI lines. Note that nitrogen is not accounted for in the model calculations, and corresponding line identifications are therefore marked with an asterisk. The feature at 4940 Å is probably a forbidden O V line (Torres & Massey 1987) not included in the model. For more details see text.

for a post-AGB star becoming a white dwarf with the standard mass of 0.6 $M_\odot$. The stellar radius R_* then follows via Stefan-Boltzmann's law $L = 4\pi R_*^2\, \sigma\, T_*^4$ from the determined stellar temperature T_*. We discuss the analyses of both program stars separately in the following subsections and compile the results in Table 2.

4.1. NGC 6751

The spectrum of NGC 6751, classified as [WC 4], shows lines from a wide range of ionization stages. Prominent features are He I 5876 Å, He II 5412 Å, C III 5695 Å, C IV 5805 Å, O V 5608 Å, O VI 3820 Å and O VI 5290 Å. As a major problem of our analysis, it is not possible to produce simultaneously C III *and* O VI lines in the same model at any parameter combination. This turned out in a comprehensive parameter study containing 69 models with stellar temperatures from T_* = 30 up to 200 kK and transformed radii R_t between 40 and 0.4 $R_\odot$. For that study the model atoms were especially extended to lower ionization stages (cf. Table 1). The spectra of all models show the lines of He II and C IV. However, lines of low ionization stages, i.e. He I and C III, occur only in models with high mass-loss rates, while the lines of high ionization stages (i.e. O V and, especially, O VI) are formed only by models with low mass-loss and temperatures higher than approximately 60 kK (O V) and 80 kK (O VI), respectively.

For NGC 6751 we present three models (cf. Fig. 2) which differ only in their mass-loss rates (i.e. the transformed radii)

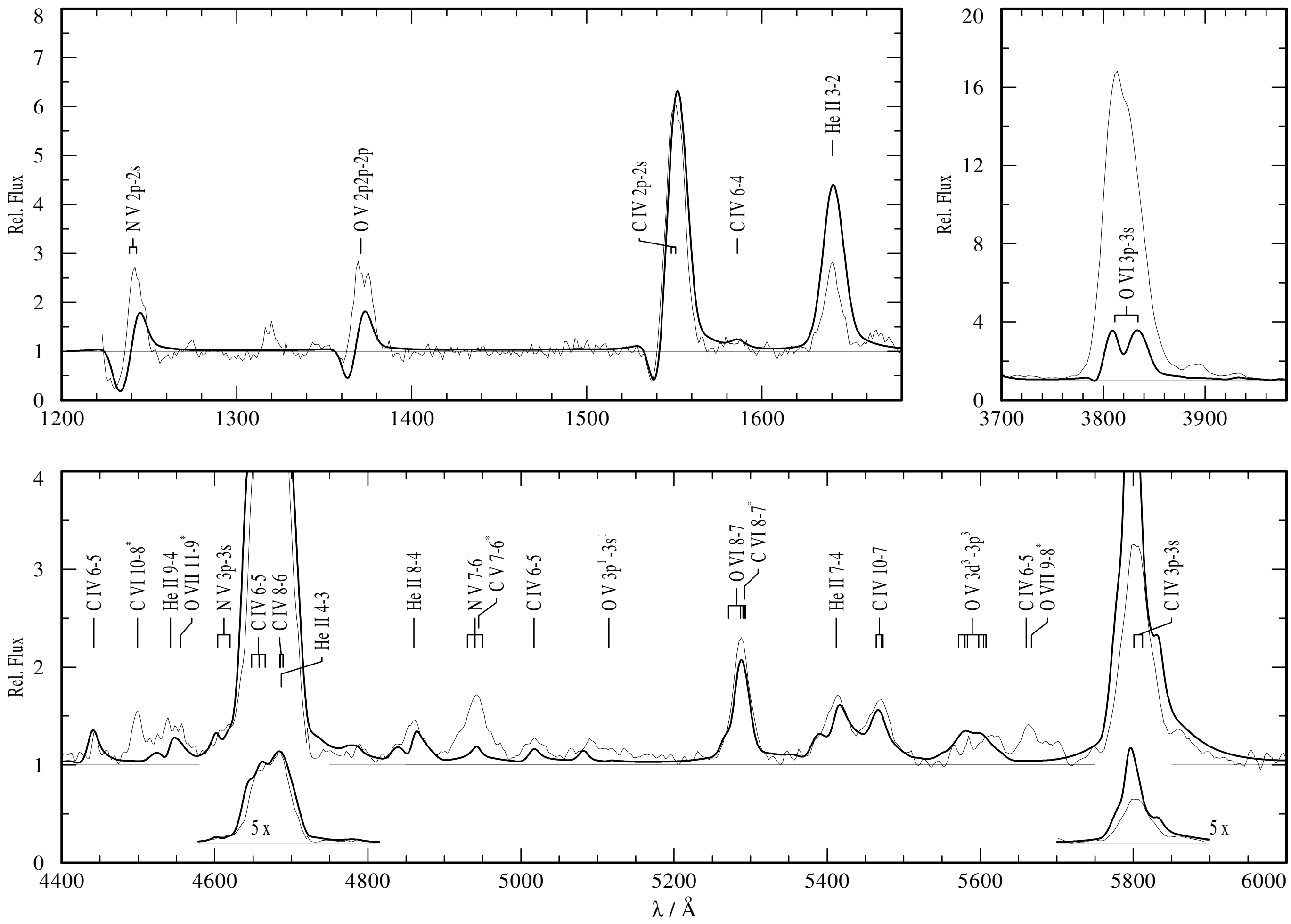

Fig. 3. Fit of Sand 3. The observation (thin lines) is shown together with the synthetic spectrum (thick lines). The fit parameters are $T_* = 140$ kK, $R_t = 3.01\,R_\odot$, $R_* = 0.12\,R_\odot$, $\log(\dot{M}/(M_\odot \mathrm{yr}^{-1})) = -6.15$, $v_\infty = 2200$ km/s, $\beta_C = 0.26$, $\beta_O = 0.12$ and $\beta_N = 0.005$ (the rest is contributed by helium). Except the strong O VI doublet at 3820 Å, the synthetic spectrum does fairly agree with the observation. Note that the lines from very high excited ions like C V, C VI and O VII (marked with an asterisk) are not formed in the photosphere and cannot be reproduced by the model (cf. Sect. 5.2).

in order to reproduce lines of all ionization stages observed. The model with the highest transformed radius R_t (low mass-loss rate) matches the O V (5590 Å) and O VI (3820, 5290 Å) lines, but no C III (5696 Å) line appears. The He II (5412 Å), C IV (5470 Å) and O V (1370 Å) lines are weaker by a factor of two than observed. The model with the lowest transformed radius (high mass-loss rate) does not fit only the He II and C IV lines but also the C III line at 5696 Å. However, in this model no O V and O VI lines in the optical range appear. Additionally the synthetic profiles of a model with an intermediate mass-loss rate is shown. This model reproduces the He II, C IV, O IV (4780 Å) and O V lines. The peak heights of the O VI lines are reached half. No C III line is seen. Compared to the dense model the ratio between the helium and the carbon line in the pair at 5412/5470 Å slightly changes. This gives an idea of the sensitivity of the carbon-to-helium ratio with respect to the model parameters.

The parameters of the three models are $T_* = 135$ kK and $R_t = 2.5$, 2.0 and $1.0\,R_\odot$, respectively. As mentioned above we calculate the stellar radius of $R_* = 0.13\,R_\odot$ from T_* assuming $\log(L/L_\odot) = 3.7$. The terminal velocity of $v_\infty = 1600 \pm 200$ km/s is estimated from comparing the width of the observed lines, in particular of C III 5696 Å, with the width of the synthetic profiles. The transformation law yields mass-loss rates of $\log(\dot{M}/(M_\odot \mathrm{yr}^{-1}))$ = -6.12, -5.97 and -5.52 for the three models, respectively.

The determination of the chemical abundances is described in the following. The helium-to-carbon ratio can be nicely derived from the neighboring lines He II 5412 Å and C IV 5470 Å. The strength of both lines changes roughly by the same amount when the parameters T_* and R_t are varied, and therefore the uncertainty is small. The influence of different mass-loss rates on the derived helium-to-carbon mass ratio is discussed in Sect. 5.4. Keeping the helium-to-carbon number ratio fixed, the oxygen abundance can be varied over a wide range without any

Table 2. Results of the analyses

Star	T_* [kK]	$T_{2/3}$ [kK]	R_t [R_*]	R_* [$R_\odot$]	$\log \dot{M}$ [$M_\odot\,\mathrm{yr}^{-1}$]	v_∞ [km/s]	$\log L$ [$L_\odot$]	β_C (mass fraction)	β_O	β_N
NGC 6751	135	55.5	2.5	0.13	-6.12	1600	3.7	0.31	0.15	-
NGC 6751	135	91.5	2.0	0.13	-5.97	1600	3.7	0.31	0.15	-
NGC 6751	135	95.8	1.0	0.13	-5.52	1600	3.7	0.31	0.15	-
Sand 3	140	96.2	3.01	0.12	-6.15	2200	3.7	0.26	0.12	0.005

dramatic changes of the synthetic helium and carbon lines. The oxygen lines grow with increasing oxygen content, but unfortunately they also react sensitively on changes of the mass-loss rate, which means that additional uncertainty affects the derived oxygen abundance. Unfortunately the most useful O IV lines in the UV region between $\lambda\lambda\,3000-3500$ are not covered by our observed spectra. Oxygen abundances up to $\beta_O \lesssim 0.25$ (mass fraction) cannot be excluded. But for $\beta_O \gtrsim 0.25$ the helium and the carbon lines would not reach the observed strength.

Unfortunately, we were not able to determine the nitrogen content in the atmosphere of NGC 6751 for two reasons. First of all it turns out that the nitrogen resonance line at 1240 Å remains nearly unchanged for nitrogen abundances between 0.005 and 0.05, and any model within this range matches the observation very well. Furthermore, the N V doublet at 4604/4620 Å in the wing of the strong C IV-He II blend is useless because the bad fit of the latter prevents reliable conclusions from the weak blends located at its wing.

The chemical composition (mass-fraction) of our best model for NGC 6751 is β_C = 0.31 and β_O = 0.15 (the complement is contributed by helium). The upper limit of the hydrogen abundance is commented at the end of Sect. 4.2. In Fig. 2 observed and synthetic spectra are compared over wide spectral ranges.

4.2. Sand 3

Originally Sand 3 was classified as a population I star of WO 4 subtype and named WR 72 (van der Hucht et al. 1981). Based on IRAS observations, van der Hucht et al. (1985) shifted Sand 3 to the group of CSPN. Because no particular WO sequence is established for the CSPN, Sand 3 is now classified as [WC 2-3] (see Sect. 5.2 for a closer discussion of its subtype).

The observed spectrum differs remarkably from that of NGC 6751. The O VI 3820 Å line is the strongest feature. In the optical spectrum no lines of the ionization stages He I, C III and O V are seen, but in the IUE spectrum the O V resonance line at 1351 Å appears. The spread of ionization stages is small, compared with NGC 6751, and one single model can reproduce almost all observed features, principally.

We find a good agreement (cf. Fig. 3) for a model with T_* = 140 kK, R_t = 3.01 $R_\odot$, R_* = 0.12 $R_\odot$, $\log(\dot{M}/(M_\odot \mathrm{yr}^{-1}))$ = -6.15 and v_∞ = 2200 km/s. As explained in Sect. 4 we calculate the stellar radius from the adopted luminosity ($\log L/L_\odot$ = 3.7). The stellar temperature and the transformed radius are derived from the analysis. The terminal velocity is obtained from comparing the line widths and has an error margin of about ± 200 km/s. Finally the mass-loss rate is calculated. The chemical abundances we derive are β_C = 0.26, β_O = 0.12 and β_N = 0.005 (the complement is contributed by helium).

The fit quality is generally good, although the strength of the oxygen doublet at 3811/3834 Å is underestimated by a factor of four. The reason for the discrepancy between this line and the O VI blend at 5290 Å is not clear. Test calculations revealed that a model which fits the doublet fails to reproduce most of the other lines. Both O V lines (at 1371 Å and around 5590 Å) are matched fairly well.

The spectrum of Sand 3 shows lines of the ultra-high ionization stages C V, C VI and O VII. This will be discussed in Sect. 5.2 in detail.

The estimation of the abundance uncertainties is the same as for NGC 6751. The helium-to-carbon ratio and the nitrogen abundance are well determined, while an oxygen abundance up to 0.25 cannot be excluded definitely, mainly because we have no observed spectra which include the useful O IV lines in the UV (between $\lambda\lambda\,3000-3500$). The influence of a varied nitrogen abundance is illustrated in Fig 4. We concentrate on this optical N V doublet because it is much more sensitive to abundance changes than the UV resonance doublet. Furthermore the continuum at 1240 Å remains uncertain at the edge of the IUE range. Four models with nitrogen abundances of 0.0, 0.005, 0.010 and 0.020 are displayed together with the observation. The model with β_N = 0.005 matches the observation in the wing of the strong He II/C IV-blend best. A nitrogen mass fraction higher than 0.010 can be excluded.

Both program stars are obviously hydrogen deficient. Test calculations for Sand 3 revealed an upper limit of $\beta_H < 0.1$ in order to remain compatible with the observed H I-Balmer/He II-Pickering decrement. In the case of NGC 6751 the limit is less restrictive due to the uncertainties in the mass-loss rate.

5. Discussion

5.1. Inhomogeneities in the atmospheres

Our models, based on the standard assumptions stationarity, homogeneity and spherical symmetry of the atmospheres, fail to reproduce all observed lines when a large spread of ionization stages occur in the observed spectra. In the spectrum of

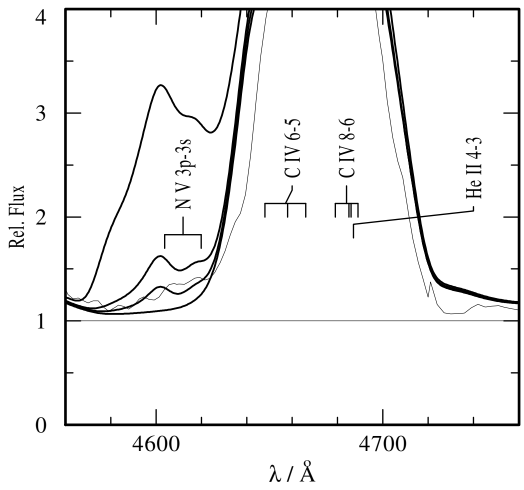

Fig. 4. The determination of the nitrogen abundance for Sand 3. Four models with nitrogen mass fractions of 0.0, 0.005, 0.010 and 0.020 are shown (thick lines) together with the observation (thin line). The model parameters are the same as given in Table 2. The strength of the N V 4604/4620 doublet at the wing of the C IV-He II blend grows with the amount of nitrogen. An abundance higher than 0.010 can be excluded clearly.

NGC 6751 one can find C III lines together with O V and O VI lines which can not be reproduced by *one* standard model. We feel that the assumption of homogeneity is not fulfilled precisely in the stellar atmospheres. Inhomogeneities, either at small or at large scales, will amplify the spread of ionization stages, principally. Low-density regions favor high ions, because the efficiency of recombination is weakened. The opposite holds for high-density regions where low ions are increased.

A first and very crude approach to a non-standard model, which accounts for inhomogeneities, is to combine two or more standard models which differ in mass-loss. For NGC 6751 we present three models of the same stellar temperature, radius, terminal velocity and chemical abundance. Two of the models, which have a low mass-loss rate ($\log(\dot{M}/(M_\odot \mathrm{yr}^{-1})) = -5.97$ and -6.12, respectively), fit the lines of the high ions (especially O V and O VI). The model with the high mass-loss rate ($\log(\dot{M}/(M_\odot \mathrm{yr}^{-1})) = -5.52$) fits the lines of the low ions (especially C III). This suggests a density contrast in the atmosphere of 0.6 dex.

Note that the electron-scattering line wings hardly differ between these three models and thus do not provide a tool for estimating the atmospheric clumpiness.

Until the development of non-standard models, which account for inhomogeneities in some appropriate way, the combination of different standard models is the only way to analyze these stars, but large error bars are implied from the uncertainty of the mass-loss rate. As a consequence the chemical composition, especially the oxygen abundance, remains uncertain because the line strengths depend on the abundances *and* on the mass-loss rate. For the determination of the helium-to-carbon ratio we use the He II/C IV line pair at 5412/5470 Å. Because the ratio (not the absolute line strengths) remains nearly unchanged when the mass-loss rate is varied, it is most reliable. The oxygen abundance, however, is much more uncertain because no line pair (He/O or C/O) can be found which behaves similar to the He/C pair. So we use exclusively the line strengths of the O V and O VI lines, which are affected by the mass-loss *and* the oxygen abundance. We achieve a lower limit of about $\beta_\mathrm{O} = 0.05$ from the fact that at lower abundances all oxygen lines would be too weak at any mass-loss rate. An oxygen abundance $\beta_\mathrm{O} > 0.25$ can be excluded because then all helium and carbon lines would appear too weak.

In the spectrum of Sand 3 the spread of ionization stages is not as pronounced as in the spectrum of NGC 6751. Thus, in terms of the explanation by inhomogeneities, we conclude that Sand 3 has a less clumpy wind for some unknown reason.

5.2. Ultrahigh-excitation lines in the spectrum of Sand 3

As reported first by Barlow et al. (1980) Sand 3 shows lines of ultrahigh ions like C V, C VI, O VII and O VIII. The same lines and additionally lines of highly ionized nitrogen and neon were identified by Werner et al. (1995) in two hot DO white dwarfs and by Dreizler et al. (1995a) in four DAO and DO white dwarfs. Werner et al. (1995) calculated line blanketed plane-parallel non-LTE models as hot as 700 kK, accounting for appropriate model atoms, to achieve lines of such high metal ions. But, as expected, no model can reproduce both the lines from ultra-high ions and from He II. Hence they conclude that the ultra-high excitation lines cannot be explained by any atmospheric model in radiative equilibrium. We think that the same holds for our spherically expanding case. Therefore we favor the hypothesis that ultrahigh ions are produced by shock heating. Due to the lack of adequate hydrodynamic models, this hypothesis cannot be verified.

Note that an ultrahigh-excitation line enters the spectral classification scheme by Méndez & Niëmela (1982). [WC 2] and [WC 3] are only discriminated by the comparison between O V 5595 and O VII 5670 (O V < O VII → [WC 2]). Following this criterion, our spectrum of Sand 3 indicates the subtype [WC 2]. However, Méndez et al. (1985) attribute the subtype [WC 3] to that star. Considering the putative non-photospheric origin of the O VII emission, we hesitate to decide that question and quote subtype [WC 2-3] for Sand 3 throughout this paper.

5.3. The nebulae

The nebula NGC 6751 (alias PN G029.2-05.9) has been studied frequently in the past (see the bibliography in Acker et al. 1992). The Zanstra temperature has been determined by de Freitas Pacheco et al. (1986) who obtained $T_Z(\mathrm{H\,I}) =$ 27.75 kK (for $T_Z(\mathrm{He\,II})$ no value is given) under the usual assumptions (especially a blackbody flux distribution). This is in remarkable contrast to the stellar temperature $T_* = 135$ kK of our model. Part of the discrepancy is due to the blackbody assumption. Our model continuum corresponds to a blackbody Zanstra temperature of 74.0 kK (H I) and 24.2 kK (He II), re-

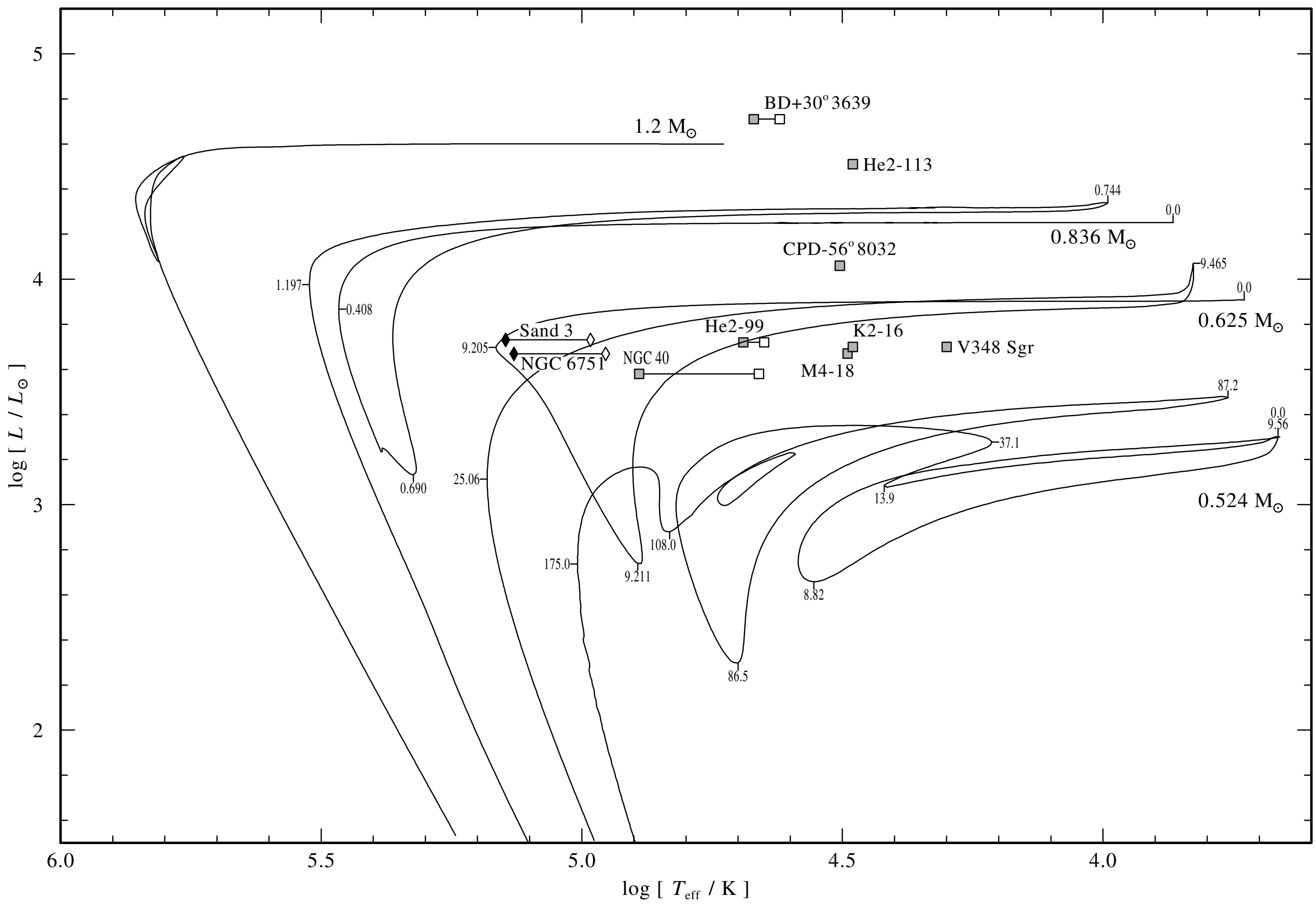

Fig. 5. Our program stars (filled diamonds) in a HR diagram with evolutionary tracks from Blöcker (1993, 1995) and Paczyński (1970) taken from Leuenhagen et al. (1996, their Fig. 14). The tickmarks on the tracks denote the time (in 10^3 yr) since leaving the AGB. The filled squares give the positions of [WCL] stars. For the two [WCE] program stars, and for NGC 40, He 2–99 and BD+30°3639, the position for $T_{2/3}$ instead of T_* is marked additionally (open symbols).

spectively. These values are much lower than T_* because of the "infrared excess" of the expanding atmosphere which enhances the visual brightness (reference photometry for the Zanstra method). The Zanstra temperature is further lowered (by 10 or 20 kK for T_Z(H I)) when line contamination increases the photometric measurement of the visual continuum. By the way, the *color* temperature of the star derived by de Freitas Pacheco et al. (1986) as low as 22.9 kK is in full agreement with our model continuum which has only a small slope in the visual due to the mentioned free-free excess at longer wavelengths.

NGC 6751 is apparently a triple-shell nebula with bipolar outflow and a faint envelope (Chu et al. 1991) showing abundance anomalies. From the Balmer decrement they derived a color excess E_{B-V} = 0.46 mag. With this reddening correction, our model flux matches the IUE spectrum and the visual photometry (de Freitas Pacheco et al. 1986) and yields a distance modulus corresponding to d = 1.3 kpc, which compares favorably with the 2.0 kpc derived by Chu et al. (1991) from the galactic kinematics of the H II region probably related to NGC 6751.

Almost nothing is known about the nebula around Sand 3. The spectrum does not show any nebular emission. No nebular image has been resolved on sky images. The only hint that Sand 3 is a planetary nebula comes from the – spatially unresolved – IR emission detected with IRAS by van der Hucht et al. (1985), as mentioned already above. Comparison with our model flux indeed confirms that the measured IR fluxes are above the stellar continuum by orders of magnitude. Based on the CPN luminosity of 5000 $L_\odot$ adopted throughout this paper, the distance of Sand 3 derived by comparing the absolutely calibrated visual and IUE spectra with the model flux while using an E_{B-V} = 1.21 E_{b-v} = 0.34 mag (which gives a slightly better fit to the IUE flux than the value quoted in Sect. 3.2) is d = 1.1 pc, well within the rough limits (0.58 ... 2.2 kpc) estimated by van der Hucht et al. (1985).

5.4. Status of evolution

Recently Leuenhagen et al. (1996) discussed the evolutionary status of WC-type central stars. In principal their discussion holds for CSPN of early WC-type as well. Summarizing, WC-type CSPN are post-AGB objects which have totally lost their hydrogen envelope. Neither evolutionary tracks for hydrogen burners nor for helium burners can explain the strong carbon enrichment as reported in this work and in Leuenhagen et al. (1996). We find $\beta_C/\beta_O \approx 0.5$ by mass for early type WC-CSPN, while Leuenhagen et al. (1996) give $\beta_C/\beta_O \approx 1.0$ for late type WC-CSPN.

The "born-again-scenario" has been proposed by Iben et al. (1983) in order to explain the carbon-rich post-AGB stars. At the Asymptotic Giant Branch, stars suffer from thermal pulses because the simultaneous burning of the hydrogen and the helium shell is unstable. After a star left the AGB and became already a central star or a white dwarf, it may suffer a "late thermal pulse" which throws it back to the AGB. Additional mass-loss then entirely removes the hydrogen-rich envelope. The born-again central star now exhibits a helium-carbon surface composition as the result of helium burning. Normally, nitrogen has been completely destroyed in those layers. However, by the last thermal pulses hydrogen might be convected downwards and reacts with carbon yielding some nitrogen ("third dredge up", Iben & Renzini 1983).

Thus, the abundance pattern observed in our program stars is in qualitative accordance with the "born-again-scenario". However, the probability of a late thermal pulse seems to be in conflict with the large fraction of hydrogen-poor CSPN.

In Fig. 5 we repeat the HR-diagram presented by Leuenhagen et al. (1996) – their Fig. 14 – augmented by our two program stars. Both stars are located near the 0.625 $M_\odot$ track. Note that the surface abundance along the theoretical tracks is dominated by hydrogen, i.e. these tracks are not adequate for explaining hydrogen deficient stars.

As Leuenhagen et al. (1996) and Hamann (1996) pointed out, an evolutionary sequence [WCL] $\rightarrow$ [WCE] $\rightarrow$PG 1159 is most likely. However, the carbon-to-helium abundances ratios we find in the studied [WCE] stars are in conflict with the ratios for [WCL] and PG 1159 stars. For the latter two groups a carbon-to-helium ratio of ≈ 1 is established (Leuenhagen et al. 1996, Dreizler et al. 1995b, respectively), while we find β_C/β_{He} = 0.4 and 0.6 for Sand 3 and NGC 6751, respectively.

In Fig. 6 we study the influence of different carbon-to-helium ratios on the line strengths in order to give a clue to the significance of the chemical abundance we derive. Two models for NGC 6751, only differing in β_C/β_{He} from 0.6 to 1.0, are presented together with the observation.

The peak height ratio between C IV 5470 Å and He II 5412 Å changes by a relatively large amount, while the changes in the oxygen lines are very small as expected. Normally we would rule out a carbon-to-helium mass ratio of 1.0 on the basis of Fig. 6, but in the special case of NGC 6751 where we need three models to match the variety of observed lines we are not as sure. As can be seen in Fig. 2 the peak height ratio between the two lines considered here changes with the mass-loss rate by at least half of the amount reported in Fig. 6. Therefore we cannot exclude safely an abundance ratio of unity for NGC 6751 which would be in agreement with the results found for the [WCL]

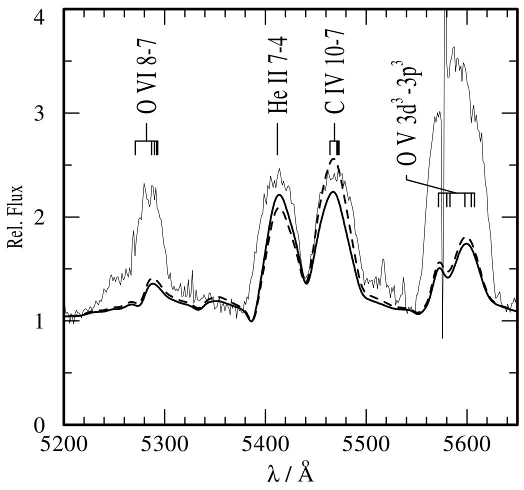

Fig. 6. Influence of different C/He ratios on the line strengths. Two models with different compositions (β_C/β_{He} = 0.6, solid line; β_C/β_{He} = 1.0, dashed line) are plotted together with the observation of NGC 6751. The ratio between the peak intensities of C IV 5470 Å and He II 5412 Å differs significantly. The changes in the oxygen lines are, as expected, very small.

and PG 1159 stars by Leuenhagen et al. (1996) and Dreizler et al. (1995b), respectively. On the other hand, for Sand 3 we are sure that a carbon-to-helium mass ratio of 1.0 is clearly outside the error margins because the observation is reproduced well by one synthetic spectrum.

5.5. Concluding remarks

The spectral analysis of two central stars with "early" WC-type spectra revealed stellar temperatures of about 140 kK and mass-loss rates of about $10^{-6} M_\odot \mathrm{yr}^{-1}$ (cf. Table 2). The surface composition is dominated by helium (about 55% by mass), with much carbon (about 30%) and oxygen (15%) and traces of nitrogen. After having lost the entire hydrogen envelope in a "late thermal pulse", these stars may evolve along the sequence [WC-late] $\rightarrow$ [WC-early] $\rightarrow$ PG 1159. Along that track the temperature increases continuously, while the mass-loss ceases when reaching the PG 1159 stage.

Acknowledgements. L.K. acknowledges support from the Deutsche Forschungsgemeinschaft under grant Ha 1455/4-2. The calculations had performed with the CRAY X-MP 216 of the Rechenzentrum der Universität Kiel and the CRAY X-MP 216 and Y-MP 2E264 of the Konrad-Zuse-Zentrum für Informationstechnik Berlin.

References

Acker A., Ochsenbein F., Stenholm B., Tylenda R., Marcout J., Schohn C. 1992, "Strasbourg-ESO Catalogue of Galactic Planetary Nebulae", European Southern Observatory, Garching bei München
Barlow M.J., Blades J.C., Hummer D.G. 1980, ApJ 241, L27
Blöcker T. 1993, Acta Astron. 43, 305
Blöcker T. 1995, A&A 299, 755
Chu Y.-H., Manchado A., Jacoby G.H., Kwitter K. 1991, ApJ 376, 150

Dreizler S., Heber U., Napiwotzki R., Hagen H.J. 1995a, A&A 303, L53

Dreizler S., Werner K., Heber U. 1995b in "White Dwarfs", D. Koester and K. Werner (eds), Lecture Notes in Physics, Springer-Verlag, p. 160

de Freitas Pacheco J.A., Codina S.J., Viadana L. 1986, MNRAS 220, 107

Hamann W.-R. 1985, A&A 148, 364

Hamann W.-R. 1986, A&A 347

Hamann W.-R. 1987, in "Numerical Radiative Transfer", ed. W. Kalkofen, Cambridge University Press, p. 35

Hamann W.-R. 1996, in "Hydrogen-Deficient Stars", C.S. Jeffery and U. Heber (eds.), ASP Conf. Series, Vol. 96, p. 127

Hamann W.-R., Koesterke L. 1993, in "Planetary Nebulae", R. Weinberger and A. Acker (eds), Proc. IAU Symp. No. 155, p. 87

Hamann W.-R., Leuenhagen U., Koesterke L., Wessolowski U. 1992, A&A 255, 200

Hayes D.S., Latham D.W. 1975, ApJ 197, 593

Hillier D.J. 1991, A&A 247, 455

Hucht K.A. van der, Williams P.M., 1987, Observatory 107, 270

Hucht K.A. van der, Conti P.S., Lundström I., Stenholm B., 1981, Space Science Review 28, 227

Hucht K.A. van der, Jurriens T.A., Olnon F.M., Thé P.S., Wesselius P.R., Williams P.M. 1985, A&A 145, L13

Hucht K.A. van der, Hidayat B., Admiranto A.G., Supelli K.R., Doom C. 1988, A&A 199, 217

Iben I.Jr., Renzini A. 1993, Ann. Rev. Astron. Astrophys. 21, 271

Iben I.Jr., Kaler J.B., Truran J.W., Renzini A., 1983, ApJ 264, 605

Koesterke L., Hamann W.-R. 1995, in "White Dwarfs", D. Koester and K. Werner (eds), Lecture Notes in Physics, Springer Verlag, p. 198

Leuenhagen U., Hamann W.-R. 1994, A&A 283, 567

Leuenhagen U., Hamann W.-R., Jeffery C.S. 1996, A&A (in press)

Méndez R.H., Niëmela V.S. 1982, in: Wolf-Rayet Stars, Proc. IAU Symp. 99, C.W.H de Loore & A.J. Willis (eds), Reidel, Dordrecht, p. 457

Méndez R., Miguel C.H., Heber U., Kudritzki R.P. 1986, in "Hydrogen Deficient Stars and Related Objects", Proc. IAU Symp. 87, K. Hunger et al. (eds), Reidel Publishing Company, p. 323

Paczyński B. 1970, Acta Astron. 20, 47

Perek L., Kohoutek L. 1967, Catalogue of Galactic Planetary Nebulae, Prague, Czech. Acad. Sci.

Schmutz W. 1991, NATO ASI Series C 341, 191

Schönberner D. 1983, ApJ 272, 708

Torres A.V., Massey P. 1987, ApJ Suppl. 65, 459

Werner K., Dreizler S., Heber U. Rauch T., Wisotzki L., Hagen H.-J. 1995, A&A 293, L75

This article was processed by the author using Springer-Verlag LaTeX A&A style file *L-AA* version 3.